

Thermal and Nonthermal Effects of Discontinuous Microwave Exposure (2.45 Gigahertz) on the Cell Membrane of *Escherichia coli*

Carole Rougier,^a Audrey Prorot,^b Philippe Chazal,^b Philippe Leveque,^c Patrick Leprat^b

Ecole Nationale Supérieure d'Ingénieurs de Limoges (ENSIL), University of Limoges, Limoges, France^a; Groupement de Recherche Eau Sol et Environnement (GRESE), University of Limoges, Limoges, France^b; XLIM CNRS, University of Limoges, Limoges, France^c

The aim of this study was to investigate the effects on the cell membranes of *Escherichia coli* of 2.45-GHz microwave (MW) treatment under various conditions with an average temperature of the cell suspension maintained at 37°C in order to examine the possible thermal versus nonthermal effects of short-duration MW exposure. To this purpose, microwave irradiation of bacteria was performed under carefully defined and controlled parameters, resulting in a discontinuous MW exposure in order to maintain the average temperature of the bacterial cell suspensions at 37°C. *Escherichia coli* cells were exposed to 200- to 2,000-W discontinuous microwave (DW) treatments for different periods of time. For each experiment, conventional heating (CH) in a water bath at 37°C was performed as a control. The effects of DW exposure on cell membranes was investigated using flow cytometry (FCM), after propidium iodide (PI) staining of cells, in addition to the assessment of intracellular protein release in bacterial suspensions. No effect was detected when bacteria were exposed to conventional heating or 200 W, whereas cell membrane integrity was slightly altered when cell suspensions were subjected to powers ranging from 400 to 2,000 W. Thermal characterization suggested that the temperature reached by the microwave-exposed samples for the contact time studied was not high enough to explain the measured modifications of cell membrane integrity. Because the results indicated that the cell response is power dependent, the hypothesis of a specific electromagnetic threshold effect, probably related to the temperature increase, can be advanced.

The interaction of electromagnetic fields (EMFs) and various life processes has been studied and debated for more than half a century. Identifying and evaluating the biological effects of microwaves (MW) is complex and controversial. Whereas one of the current theories is that heat generation induced by microwaves is responsible for biological effects, there has been a persistent view in the physical and engineering sciences that microwave fields are unable to induce bioeffects other than by heating (1) (2). Because of the scarcity of information on the mechanism of interaction between microwave and biological systems, this controversy endures.

A great number of studies of the thermal versus nonthermal bioeffects of low-power MW were performed with various cellular functions, including gene expression (3) and mutation (4), enzyme activity (5), unfolding of proteins (6), biochemical cell systems (7), cell wall (8), cell morphology (9), and cell proliferation (10–13). Whereas several authors showed nonthermal effects, safety standards have been set based solely upon the thermal effect of MW. The main reason was that no satisfactory mechanism was proposed to explain the nonthermal bioeffects.

When applied at high power, MW bioeffects induced by heating constitute one of the modern approaches for sterilization and decontamination processes in the food industry. In fact, microwaves have long been known to induce a rapid rise of temperature due to intermolecular friction (14, 15). Several studies which have dealt with the effect of microwaves on microorganisms (16–21) showed that the bactericidal effect of microwaves was due to thermal mechanisms. However, possible nonthermal effects of microwaves on biological systems had been discussed in numerous reports. Some authors (22–25) have mentioned nonthermal or enhanced thermal effects of microwaves, while others (26, 27) have refuted the nonthermal effects of microwaves.

One of the main reasons for these conflicting conclusions, for

either low- or high-power MW, is the difficulty in keeping and controlling isothermal conditions during MW irradiation.

In order to understand the mechanisms of interaction between MW and microorganisms, this study was designed using accurately controlled experimental conditions and well-defined MW exposure parameters. Moreover, in order to clearly differentiate thermal and nonthermal MW effects, temperature distributions have been carried out with the discontinuous-microwave (DW)-exposed cell suspension, and the finite difference time domain (FDTD) method was used to determine the specific absorption rate (SAR) spatial distributions in the tube (28). In this study, the bacterial effects of microwave irradiation were investigated using flow cytometry (FCM) in conjunction with propidium iodide staining to monitor cellular viability in addition to the assessment of intracellular protein release in bacterial suspensions.

MATERIALS AND METHODS

Bacterial strain and culture conditions. An indigenous strain of *Escherichia coli*, initially isolated from the municipal wastewater of the city of Limoges, France, was used throughout this study. It presented the following physiological characteristics: nonsporulating mobile Gram negative, cytochrome *c* oxidase negative, capable of aero/anaerobic growth, and exhibiting the API 20E profile 5044 552.

A starter culture of *Escherichia coli* was grown on a rotary shaker (250 rpm) at 37°C for 12 h to late exponential phase in peptone water (Difco;

Received 13 March 2014 Accepted 23 May 2014

Published ahead of print 6 June 2014

Editor: J. L. Schottel

Address correspondence to Audrey Prorot, prorot@ensil.unilim.fr.

Copyright © 2014, American Society for Microbiology. All Rights Reserved.

doi:10.1128/AEM.00789-14

Becton, Dickinson, MD, USA), containing 10 g/liter peptone and 5 g/liter sodium chloride at pH 7.4. The cell concentration was estimated by measuring the absorbance at 580 nm and adjusted to 10^8 cells/ml using sterile culture medium. Five milliliters of this bacterial suspension was used for conventional heating (CH) and discontinuous microwave (DW) exposure.

Microbiological studies. (i) Measurement of cell culturability. Culturability of bacteria of each sample was evaluated by the plate count method. After serial dilutions in a sterile phosphate-buffered saline (PBS) solution, 0.1-ml aliquots of the dilutions were inoculated into aerobic plate count agar (Difco, Detroit, MI, USA). Each dilution was spread in triplicate. CFU were then determined after incubation at 37°C for 24 h. Each result was the arithmetic mean from triplicates.

(ii) Cell staining and flow cytometry analyses. For flow cytometry, exposed and control samples were diluted in PBS buffer to obtain a 10^6 cells/ml suspension.

PI staining. Cells were stained using propidium iodide (PI) (Molecular Probes, Eugene, OR, USA), a DNA binding probe (molecular weight, 668.4). Since it could diffuse into cells only if their membranes are damaged, PI is also considered a valuable probe for the evaluation of membrane integrity (29). A stock solution of PI was prepared at a final concentration of 0.5 mg/ml in distilled water and was stored in the dark at 4°C. PI was added to bacterial suspensions at a final concentration of 25 µg/ml during CH or DW treatments or immediately after exposure depending on the type of experimentation. Cells suspensions were incubated in the presence of the probe for a total time of 5 min at room temperature before cytometry analyses.

Flow cytometry analyses. Flow cytometry analyses were performed using a FACSVantage cell sorter (Becton, Dickinson, MD, USA) equipped with a 488-nm (excitation wavelength of PI) argon laser. PI red fluorescence was collected with a long-band-pass filter, and bacterial green autofluorescence was collected with a 530-nm-band-pass filter. Four parameters were recorded: forward scatter (FSC), related to cell size, side scatter (SSC), related to cell structure, red fluorescence of PI, related to cell membrane integrity, and green autofluorescence of bacteria. The results were analyzed with red versus green fluorescence cytograms, since bacterial green autofluorescence enables a better bacterial population separation from background noise and cellular debris than FSC or SSC. FSC and fluorescences were collected in a 4-decade logarithmic scale, whereas SSC was collected in linear scale. The photomultiplier voltage was chosen such that control suspension (untreated *Escherichia coli* suspension) had no red fluorescence above the first decade. A minimum of 10,000 cells were analyzed at a flow rate of approximately 500 cells/s.

Measuring protein leakage. The amount of protein released from the DW- and CH-treated cells was measured after adaptation of the Bradford method (30) at 595 nm using the Bio-Rad protein assay dye reagent (Bio-Rad S.A., Germany). Bovine serum albumin was used as the standard protein. After treatment (CH or DW exposure), an aliquot of 1 ml was centrifuged at 9,000 rpm (Biofuge Fresco; Heraeus Instruments, Germany) and subjected to protein measurement.

CH. CH was performed in a shaking water bath (model A120T; Lauda, Germany) at 37°C ± 1°C. As for DW exposure, glass tubes containing 5 ml of bacterial suspensions were used. The temperature of the cell culture in the test tube was routinely measured by a Teflon-coated thermocouple (CTX 1200; Avanteq, France). The time needed for the cell suspension in the water bath to reach 37°C from room temperature was determined to be 75 s using the fluoroptic probe (model 501; Luxton, California, USA). The test tube was regularly gently shaken.

Microwave exposure. (i) Exposure system. The DW exposure system (Fig. 1) consisted of a function generator (model 33120A; Agilent, California, USA) (G1), a 2.45-GHz-microwave generator (model GMP 20KE/D; Sairem, France) (G2) containing an internal cooling system for the magnetron, and an isolator (IS) with another cooling system for dissipating the reflected power and protecting G2, a bidirectional coupler (BC) with two power meters: PM1, which measures incident power (Pi),

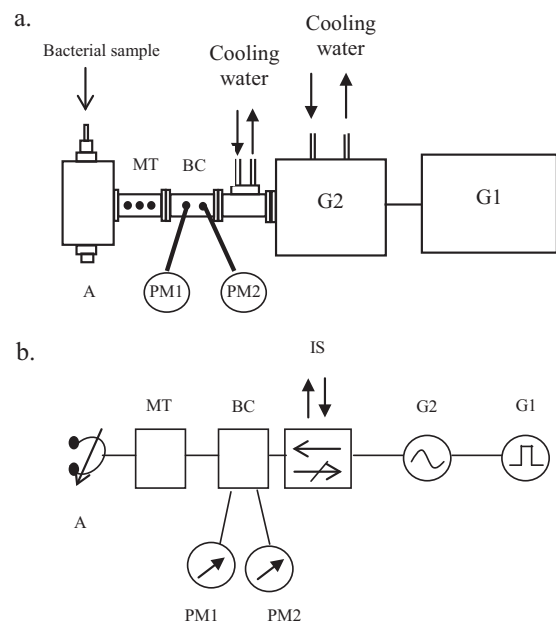


FIG 1 Schematic principles of the experimental DW exposure system. (a) Scheme of the experimental device. (b) Main components: function generator (G1), 2.45-GHz microwave generator (G2), isolator (IS), bidirectional coupler (BC), power meters (PM), and applicator (A).

and PM2, which measures reflected power (Pr). A metallic cylindrical cavity (A) (Fig. 2) was used to expose the samples. Five milliliters of bacterial suspension was exposed in glass tubes.

Due to cavity dimensions, a transverse electric TE_{111} mode was excited. It presented maximum E-field values in the center of the cavity when the cavity was empty. The resonant frequency was adjusted by changing the cavity height (after screwing two dumbbells). A good isolation was obtained using quarter-wavelength transitions (30.5 mm). The cavity was fed by a rectangular wave guide (WR340; size, 86 by 43 mm) through a circular aperture. A manual tuner (MT) (A13SMA 2450/340; Sairem, France) was used to match the system and reduce the standing wave ratio (SWR).

The test tube was placed inside the cavity through a circular aperture centered in the dumbbell. The cutoff frequency of the wave guide defined by this aperture was higher than the working frequency (2.45 GHz), and the evanescent wave was strongly attenuated because of the dumbbell length.

(ii) Microwave sequence exposure conditions. The function generator (G1) was programmed to deliver repetitive square wave pulses. Sequences for DW exposure were defined according to the microwave power and the average final temperature desired (37°C). They involved the two following stages: an initial heating exposure phase (H), necessary to rise from room temperature to 37°C, and a second phase, required for maintaining the average temperature at 37°C, corresponding to repetitive sequences of exposure (E) and nonexposure (NE). A 2.45-GHz continuous-wave (CW) microwave process was used during H and E phases.

This technology, being an original example of this operating system (including temperature evolution and duration of the different phases), will appear in Results.

The temperature of the cell culture in the glass test tube was routinely measured with a Teflon-coated thermocouple (CTX 1200; Avanteq, France). Temperature measurements were done both before exposure and immediately after gentle shaking following the exposure. As shown in Fig. 3, the maintenance of temperature at 37°C was not strictly obtained, and this parameter effectively varied between 37°C and a little more than 35°C.

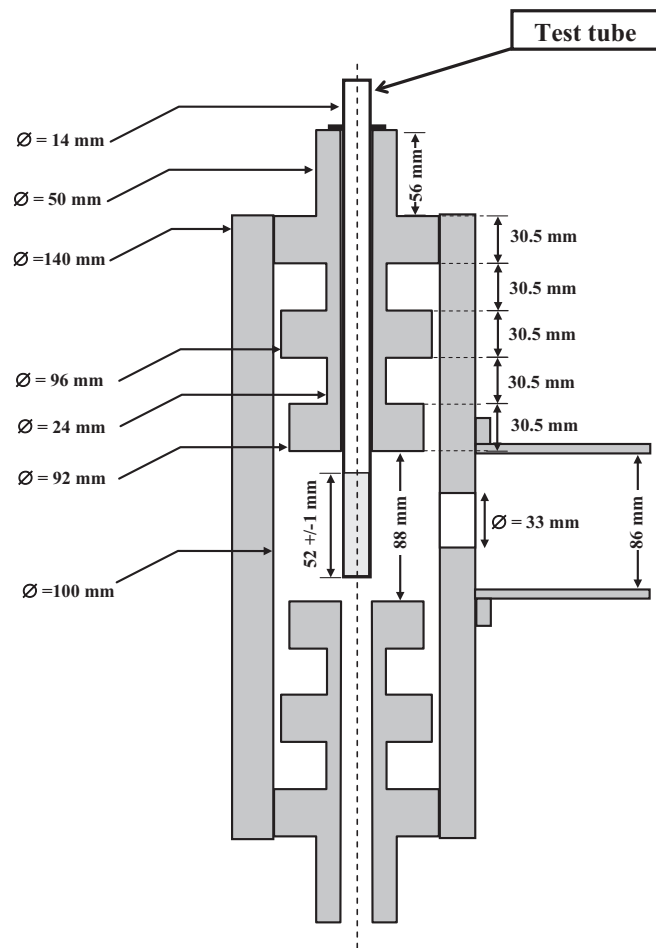


FIG 2 Schematic drawing of the cylindrical applicator containing the test tube and of the waveguide R26 (86 mm by 43 mm).

Control cells and sham exposed cells were maintained at room temperature (20°C) and gently sequentially shaken. For CH experiments, sham-exposed cells were placed directly in the metallic cavity in the absence of microwave exposure.

(iii) **Convention of writing for the expression of heating exposure times.** As appearing in Results and Discussion, the heating duration corresponds to the total heating length. In the case of DW, the convention for expressing exposure duration is more subtle. For a given experiment, the total exposure time (TE) (considered as duration) is given by equation 1:

$$TE = H + n \times (NE + E) \quad (1)$$

where H is the preliminary temperature increase duration under microwave exposure necessary to reach 37°C from room temperature, NE is the no-exposure period duration, E is the microwave exposure period duration, and n is the number of times when the sequence ($NE + E$) was made.

Thermal characterization. Thermal characterization of exposed cells was performed using a fluoroptic thermometer (model 501; Luxtron, California, USA). This system is based on a fluoroptic fiber optic sensor to measure temperature. It is immune to electromagnetic fields, and the probe is dedicated for temperature control of microwave processes and for temperature gradient mapping of fast temperature ramps. Typically, the response time is 0.25 s in stirred water, and the fluoroptic sensor, located at the end of the optic fiber, has a diameter of 0.8 mm and a thickness of 0.2 mm. Four samples were recorded per second for temperature measurement. These characteristics allow measuring a temperature in a volume that can be estimated around 1 and 2 mm³. In a previous

study, we have estimated a 200-mK standard deviation for the temperature measurement (31), and we have demonstrated the ability of this probe to measure this parameter in small volumes. It was used to compare computational and experimental estimates of the specific absorption rate (SAR) distribution in a chamber containing a volume of 0.5 ml of Hanks buffered salt solution (HBSS) (2-mm height) exposed to microwaves (32).

Point-to-point thermal measurements were carried out over the 3 dimensions of the tube volume with 1- or 2-mm spacing along the height of the sample and 3-mm spacing in the two other dimensions. For each measurement, the bacterial sample was maintained at room temperature (20°C) and the temperature was recorded during the initial exposure phase (H) and for 1 min after the end of H (i.e., during NE phase). The spatiotemporal distribution of temperature was monitored in the cell suspension for exposure of 200, 400, 800, 1,400, or 2,000 W.

Dosimetry. The finite difference time domain (FDTD) method (33–35) was used to determine the electromagnetic field and the SAR distributions in the tube as described in a previous study (28). The electromagnetic field is calculated using the FDTD method applied to Maxwell's equations. The time-dependent equations were solved using space and time derivatives. The FDTD algorithm is based on a space grid where the electromagnetic field components were computed at each time step in the whole discretized volume. A criterion linking time step and spatial grid is used for algorithm stability. If needed, the free space can be considered using the highly effective, perfectly matched layer (PML) (36). The shortest wavelength of the spectrum is required to be at least 10 times as great as the spatial grid size for appropriate spatial discretization. At 2.45 GHz, the wavelength is 12.2 cm in free space and around 1.5 cm in the solution, where the relative dielectric permittivity is around 75 (depending on the temperature). The finest resolution used was 0.33 by 0.33 by 0.33 mm. The waveguide, matching system, metallic cylindrical cavity, and coupling aperture were simulated. The excitation was done with a rectangular waveguide. The dielectric parameters used in this study were those of a typical aqueous medium. At 2.45 GHz and 37°C, the biological medium was simulated with a relative dielectric permittivity of 75, a conductivity of 2.85 S/m, and a density of 1,000 kg/m³. The glass material of the tube was modeled as lossless with a relative permittivity of 7.5. The computations were performed on a NEC SX8 vectorized supercomputer.

To quantify the amount of power absorbed per unit of mass of the solution, the specific absorption rate (SAR), expressed in W/kg, can be computed from the electromagnetic field with equation 2:

$$SAR = \frac{\sigma |E|^2}{\rho} \quad (2)$$

where E is the electric field (E-field) amplitude (V/m), σ is the electrical conductivity (S/m), and ρ is the density (kg/m³). In each elementary cell, the E field and the SAR were computed. The calorific dissipated power (σE^2 in W/m³) is directly proportional to the SAR and induces temperature elevation.

Data analysis. Exposures were compared with simultaneous sham and control cells in both cases. All the results presented in this study come from a minimum of four independent experiments. Assays on cell properties (culturability, membrane integrity, and protein leakage) for control cells, sham-exposed cells and CH- or DW-exposed cells were performed for 9 independent experiments with 5 measures per experiment. All data are expressed as means \pm standard deviations (SD). For group comparison, the analysis of variance (ANOVA) test was used. According to the weakness of microwave nonthermal effects and experimental facilities, statistical significance was defined as a P value of <0.01 . Statistical analyses were carried out using the software program SYSTAT version 13.0.

RESULTS

Elaboration of an accurate technology based on discontinuous exposure for studying the impact of microwaves on a bacterial population at constant sublethal temperature. A new technological approach was elaborated to study the effect of MW exposure

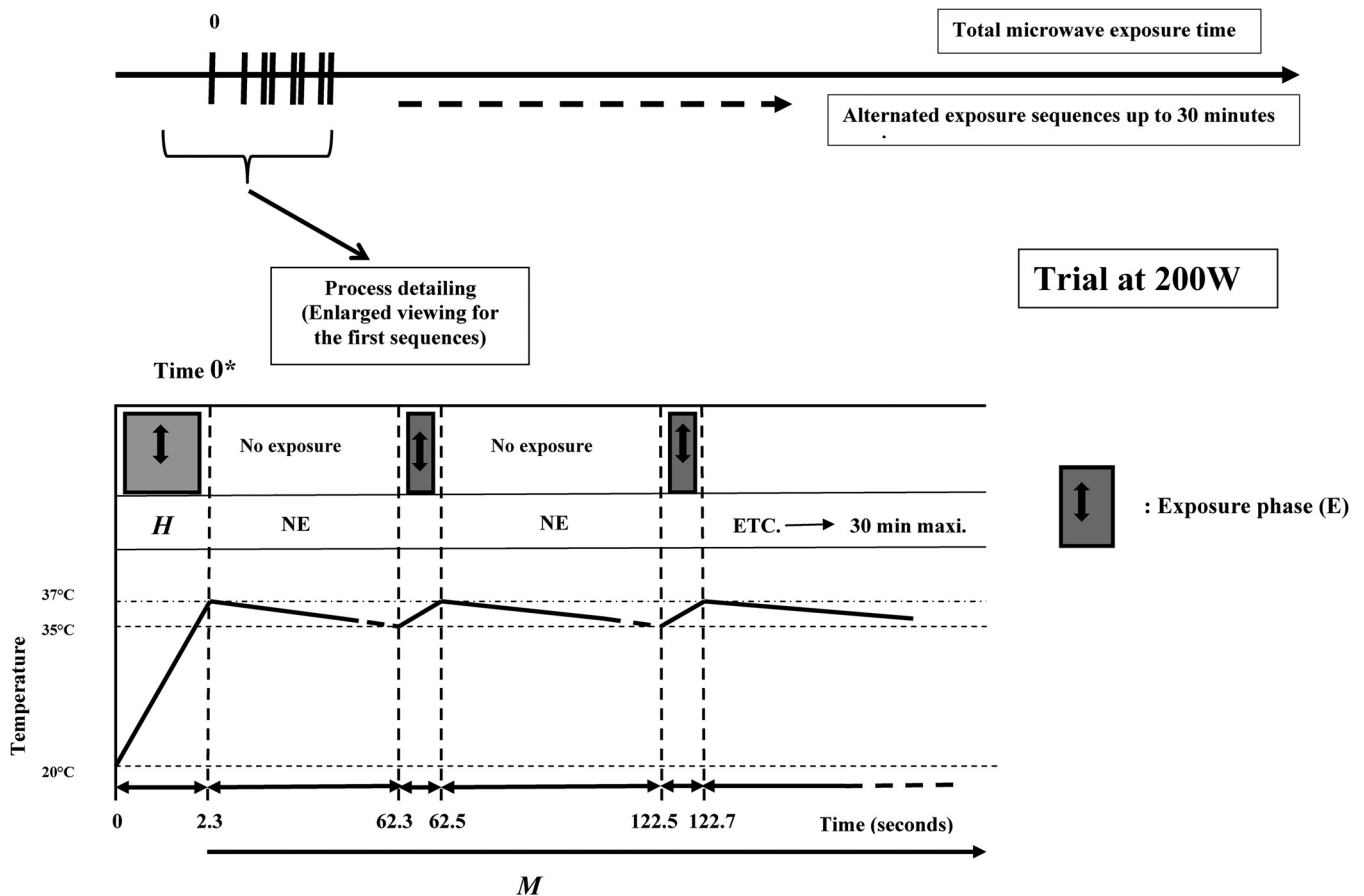


FIG 3 Protocol for DW exposure at 37°C. The description corresponds to a 200-W exposure power. The experimental procedure remains the same for the other exposure powers studied, with the exception of the phase durations, which varied from a given power to another. H, heating phase for rising from room temperature up to 37°C; M, temperature was maintained between 35 and 37°C during this phase. The M phase consisted of two subphases: NE, a nonexposure phase, and E, an exposure phase.

at a quasicontant and sublethal temperature, as previously described in Materials and Methods. An example of temperature variations in parallel with time evolution appears at Fig. 3. At 200 W, the H phase duration was 2.3 s. At the end of this phase, the temperature reached 37°C. A no-exposure phase (NE) followed (60 s). The temperature progressively decreased to 35°C. A 0.2-s MW exposure phase (E) was sufficient to increase temperature to 37°C. Another NE phase followed, etc. The addition of NE + E phases constituted the global (M) phase. M phase varied from 0 to 30 min in the range from 0* to 5 to 10 to 20 to 30 min. 0* is the initial time for M phase, corresponding to the end of H phase. At time zero*, the physiological state of cells is the one resulting from the impact of a rapid temperature increase during H phase.

Table 1 shows the variations of H phase duration (for a constant nonexposure [M] period fixed at 60 s) when the MW power varied from 200 to 2,000 W. This table also shows that the duration of H and E phases evolved as a function of time in a quasi-inversely proportional mode.

Macroscopic biological investigations of microwave DW exposure. The effects of DW exposure on *Escherichia coli* were compared to the ones obtained after conventional heating (CH) in a water bath at sublethal temperatures (Table 2). Whatever the exposure mode, and after pour spreading on agar plates, no apparent death was noticed at 37°C for contact times increasing up to 30

min and for microwave power values (in the case of DW) varying from 200 to 2,000 W. In addition, another parameter was studied, the amount of protein released in the medium, since the leakage of cell components could be an indicator of the loss of membrane integrity. Exposure to CH in a water bath or to DW induced no statistically significant effect on protein leakage, regardless of the microwave power and the exposure time at least in the case of DW investigation. Membrane damage, if any, at this temperature and under these conditions could be repaired, showing a little impact of exposure on cellular revivification.

Physiological approach of *Escherichia coli* sensitivity to DW and CH at sublethal temperature. The physiological state of the bacterium differed according to the mode of exposure at the tem-

TABLE 1 Duration of DW exposure at 37°C

Phase ^a	Duration (s) of exposure to:				
	200 W	400 W	800 W	1,400 W	2,000 W
H	2.3	1.15	0.575	0.328	0.23
NE	60	60	60	60	60
E	0.23	0.11	0.05	0.028	0.02

^a "H" corresponds to the heating phase, "E" to exposure, and "NE" to nonexposure phases ("E" + "NE" correspond to the M phase, which maintains the temperature).

TABLE 2 Effects of DW exposure and conventional heating on culturable cell concentration and protein leakage in comparison with results for the control (sham-exposed cells)

Parameter	Control cells		Sham-exposed cells		CH-exposed cells		DW-exposed cells	
	0	30	0	30	0	30	0	30
No. of CFU/ml	$1 \times 10^8 \pm 1 \times 10^7$	$9 \times 10^7 \pm 1 \times 10^7$	$1.1 \times 10^8 \pm 1 \times 10^7$	$1 \times 10^8 \pm 1 \times 10^7$	$1.8 \times 10^8 \pm 1 \times 10^7$	$1.9 \times 10^8 \pm 1 \times 10^7$	$1.2 \times 10^8 \pm 1 \times 10^7$	$1.1 \times 10^8 \pm 1 \times 10^7$
Concn of leaked proteins ($\mu\text{g/ml}$)	0.31 ± 0.03	0.30 ± 0.03	0.35 ± 0.04	0.38 ± 0.04	0.51 ± 0.05	0.48 ± 0.05	0.41 ± 0.04	0.44 ± 0.04

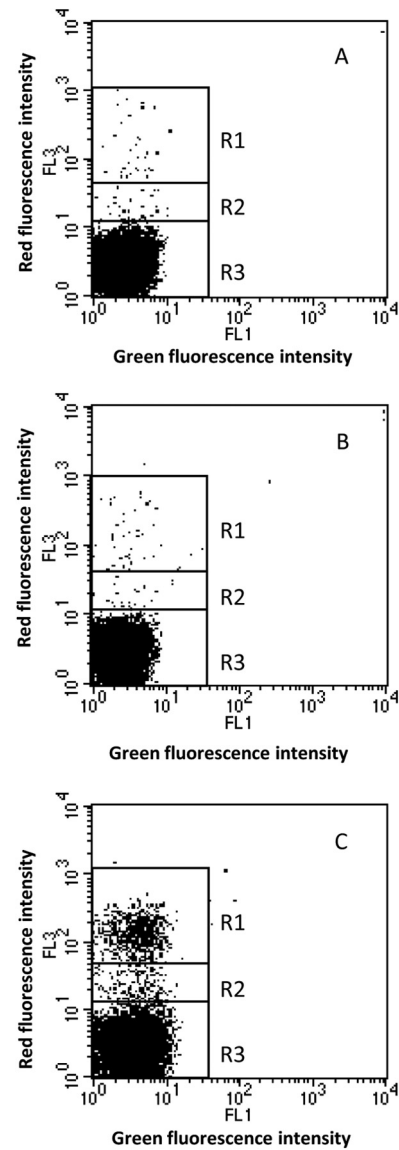


FIG 4 Cytograms for untreated (A), conventionally heated (B), or 400-W-DW treated (C) *Escherichia coli* suspensions stained with PI. The cytogram (A) corresponds to control cell suspension maintained at room temperature. Cell treatments for panels B and C were performed at 37°C during the heating phase (temperature increase from room level up to 37°C). Windows R1, R2, and R3, respectively, corresponded to highly, low-level-, and no PI-stained cells.

perature of 37°C, and noticeable differences appeared when the contact was realized under CH or under DW (Fig. 4). Cell membrane integrity was assessed using propidium iodide (PI) incorporation detected by FCM. PI is a DNA binding probe that diffuses only into the cells with a damaged membrane. Specific PI-DNA binding then results in a red fluorescence emission that can be detected by FCM. As a positive control, a conventional heat-treated sample (95°C during 15 min) was used. The FCM analyses reveal around 100% of permeabilized cells after heat treatment (data not shown).

An example of the cytograms of the different samples obtained after FCM analysis in conjunction with PI appears in Fig. 4. Cyto-

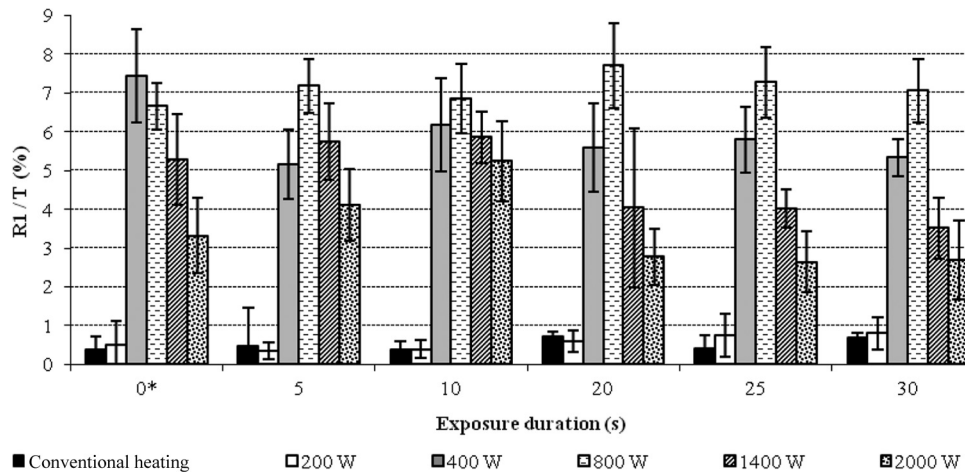


FIG 5 Evolution of $R1/T = f(W)$ for different exposure times. Time 0^* corresponds to the time required for increasing the temperature to room level up to 37°C . In other terms, 0^* is the length of the H phase, which varied from a given W (exposure power) value to another. T , total population.

gram A corresponds to a control cell suspension maintained at room temperature. Cell treatments for cytograms B and C were performed at 37°C during the heating phase (increase from room temperature to 37°C) with conventional heating (B) or DW heating (C) (400 W in this example).

Red versus green fluorescence intensities showed clearly three cell populations after DW exposure: a highly PI-stained cell population (R1), a low-level-PI-stained cell population (R2), and a no-PI-stain cell population (R3). The cell response to temperature exposure varied according to the contact mode. Cell suspension at 37°C with CH exhibited 0.4 to 0.7% of R1 permeabilized cells regardless of the exposure duration (Fig. 4 and Fig. 5). Under such conditions, no statistically significant differences of membrane integrity were found compared to results obtained with control and sham-exposed cell suspensions maintained at room temperature, which exhibited 0.3 to 0.5% of R1 cells (Fig. 4A).

DW exposure induced approximately 8% of R1 cells at the maximum (Fig. 4C and 5). Variations in results were statistically significant ($P = 0.001$) from 400- to 2,000-W exposure. For all exposure durations, the percentage of R1-permeabilized cells was slightly greater for bacterial suspensions exposed to 400 or 800 W than for suspensions exposed to 1,400 or 2,000 W (Fig. 5). No statistically significant effect on cell permeability was detected for 200-W-DW exposure compared to results with CH treatment.

By adding both R1 and R2 cell levels, 9 to 10% of cells with modified membrane integrity were found for a 400-W-DW exposure (Fig. 4A), whereas only 0.8 to 1% of cells of the same type were recorded for a 200-W-DW exposure (Fig. 4B) or after CH and 0.5 to 1% for control and sham-exposed cells maintained at 20°C . Control and sham-exposed cells maintained at 20°C exhibited only 0.5 to 1% of membrane-permeabilized cells.

Results shown in Fig. 4 were obtained after a contact time (TE) of 5 min. Increasing exposure times up to 30 min did not induce any increase in the percentage of permeabilized cells (Fig. 5). Thus, the H phase appeared to be the most responsible for the measured effects of microwaves on the membrane integrity. Moreover, when a cell suspension previously heated at 37°C under the conditions of CH was then immediately subjected to the M phase under DW conditions, no effect on membrane integrity was seen even after a 15-min contact time. Since it is known that mi-

crowaves effects are heterogeneous when applied to living cells or organisms (2, 6–9, 37), the hypothesis of local superheating within the *E. coli* population during the H phase was suggested. In order to determine at which temperature a biological denaturation effect begins to occur, with close to the 8% of R1-permeabilized cells obtained after DW exposure, as appearing at Fig. 4, the effect of increasing temperature in CH conditions was studied. The results showed that conventional heating at 47°C for 10 min or at 48°C for 5 min was necessary to induce approximately the same effect as DW exposure (Fig. 6).

Approaching the DW/CH exposure consequences for *Escherichia coli* cells in a thermic respect. The SAR distribution was investigated using FDTD numerical simulation in order to characterize the microwave exposure conditions. Simulation of SAR distributions in a DW-exposed cell sample showed a great heterogeneity: simulated SAR could reach 0.89 W/g at the maximum for 1-W incident power (Table 3).

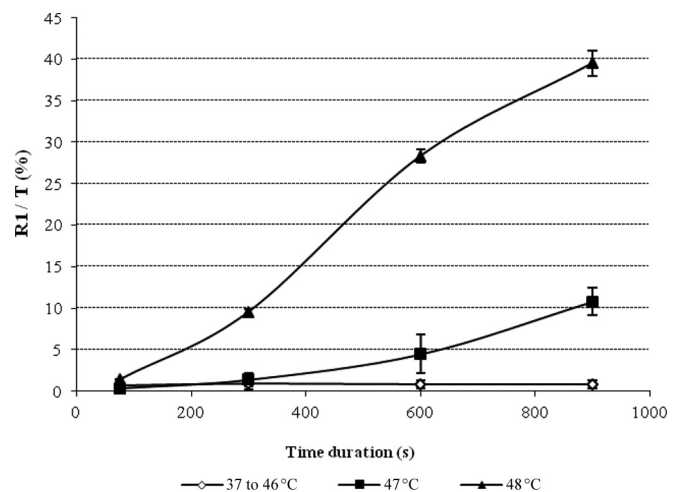


FIG 6 Effect of conventional heating at different temperatures on membrane permeability. Results are expressed as the evolution of $R1/T = f(t)$ for different T ($^\circ\text{C}$) values (where t is time). The curve named “37 to 46°C ” corresponds to the average value of the results obtained at 37, 40, 42, 45, and 46°C , since percentages of highly stained cells were similar.

TABLE 3 Simulated SAR values in the tube exposed in the metallic cylindrical cavity for 1 W of incident power^a

Parameter	Mean	SD	Max	Min
SAR, W/g for 1 W	0.189	0.198	0.89	4.10^{-4}
E, V/m for 1 W	364	373	790	5.3

^a Max, maximum value; Min, minimum value.

The spatial SAR distribution is presented in Fig. 7. In order to illustrate the SAR distribution in the whole medium, a three-dimensional (3D) view of the solution and slices along the test tube was plotted. It can be observed that the SAR distribution is not homogenous and highlights two SAR hot spots near the top and the bottom of the test tube, where the maximum SAR values are obtained.

During the initial phase (H), SAR peak values were very high, ranging from 38 W/g for 200-W incident power up to 380 W/g for 2,000-W power (Table 4). In the M phase, the whole-volume SAR reached 0.125 W/g (125 W/kg), averaging values over the time for all applied incident powers (Table 4). Nevertheless, this phase did not induce any temperature rise due to the temperature difference between the cell sample (at an approximate average temperature of 37°C) and the surrounding atmosphere in the cavity (approximately at room temperature). For both treatments (CH or DW), the numeration of culturable cells on nutrient solid medium after treatment did not show any statistically measurable cell mortality (data not shown).

Because modifications of the cell membrane integrity after cell exposure might be attributed to localized thermal effects, further investigations were carried out to search for the existence of ther-

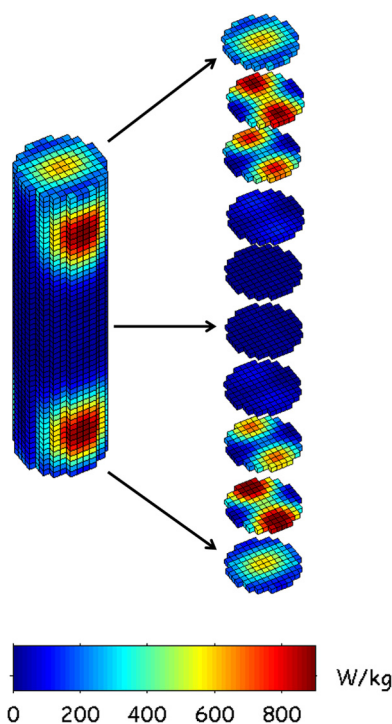


FIG 7 3D SAR distribution: whole-volume and 5-mm slices. In this view, the FDTD spatial resolution was 1 mm^3 , and the SAR values were normalized for 1-W incident power.

TABLE 4 Simulated SAR values for the heating phase (H) and the phase which maintains temperature (M) according to the exposure time duration

Phase	Parameter	Value at incident power (W)				
		200	400	800	1,400	2,000
H	SAR peak (W/g)	38	76	152	304	380
	Time duration (s)	2.30	1.15	0.575	0.287	0.23
M	SAR mean (W/g)	0.125	0.125	0.125	0.125	0.125
	Time duration of E (s)	0.23	0.115	0.0575	0.0287	0.023

mal hot spots in the cell suspension. Temperature measurements were carried out with DW-exposed samples during H and NE phases, corresponding to 1-min acquisition. The spatiotemporal temperature distributions were similar for the different power levels (200 to 2,000 W). Figure 8 represents the temperature distribution along the central axis of a 400-W-DW-exposed sample. The results showed a heterogeneous spatiotemporal distribution of temperature: the top of the cell suspension was warmer than what was observed at the bottom of the last one (Fig. 8). However, the cooling time rate was shorter at the bottom than at the top of the suspension, probably because of the existence of convection phenomena. A rapid rise of temperature during this H phase was observed in all measured sampling points. Nevertheless, point-to-point measurements over the three dimensions of the sample volume did not show the presence of localized thermal hot spots corresponding to temperatures higher than $45 \pm 1^\circ\text{C}$ after the end of H phase. The area containing the measurement spots higher than 37°C was located approximately between 0 and 8 mm below the meniscus of the cell suspension (Fig. 8). The SAR hot spots induced a temperature gradient, and considering thermal phenomena, conduction, and especially convection, this heterogeneity causes a significant fluid motion, as illustrated in the experimental measurements and numerical simulation, including the fluid velocity in the heat transfer equation (28). This analysis supports the concept that SAR hot spots do not directly induce thermal hot spots, as illustrated in the temperature measurements (Fig. 8).

DISCUSSION

Despite many studies on effects of low- and high-power MW on biological systems, the mechanism responsible for the observed bioeffects remains uncertain. Because of the lack of information on the mechanism of interaction between microwave and biological systems, a low-temperature process based on DW energy was developed to investigate their effects on microorganisms under sublethal conditions.

Our results showed that DW exposure at 37°C did not induce any significant *E. coli* mortality (culture on solid medium) but had an effect on membrane integrity (PI staining) of a small part of the bacterial population. Indeed, we found approximately 8% of R1-permeabilized cells after exposure, while conventional heating at 37°C did not induce any effect on membrane permeability compared to that of untreated cell suspensions. Moreover, it can be noticed that conventional heating at 47°C for 10 min or at 48°C for 5 min was necessary to induce the same effects. From these results, it is not possible to establish a direct link between the effect on membrane permeability and a temperature increase after micro-

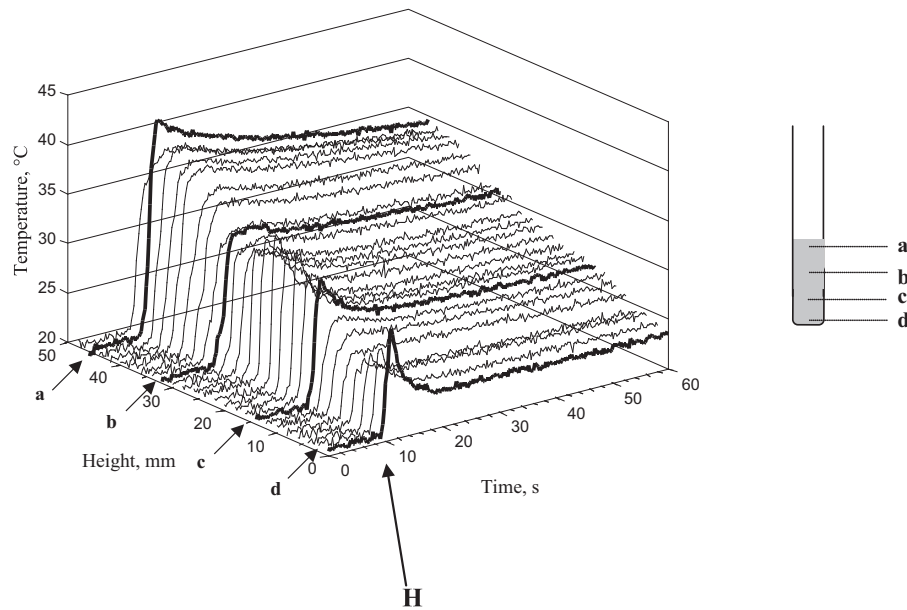


FIG 8 Spatiotemporal distribution of temperature along the central axis of the test tube after cell suspension exposure at 400 W during the heating phase (H) and 1 min after.

wave exposure. The challenge in investigating the specific effects of microwave exposure on microorganisms at sublethal temperatures involves the inherent difficulty in measuring the temperature of a sample during microwave processing and the inaccuracies in measurement that can result (9). For this reason, this study was designed using accurately controlled experimental conditions and well-defined microwave parameters. Special attention was paid to temperature measurements using a fast-response probe immune to electromagnetic fields, which integrates temperature on a volume of the order of cubic millimeters with a time resolution shorter than 0.25 s. Under these experimental conditions, thermal characterization during the heating step clearly revealed a heterogeneous temperature distribution in the cell suspension, but no spots above $45 \pm 1^\circ\text{C}$ were measured over the cell suspension volume.

Moreover, if the observed membrane damage was the consequence of a thermal effect, these effects would be observed regardless of the applied powers (with a temperature increase around 17°C in the H phase). In our study, the cell response is power dependent: no effect was observed at 200 W, whereas significant effects were pointed out for power equal to or higher than 400 W. No more severe damage related to the applied power increase was observed over 400 W. From these results, the hypothesis of a specific electromagnetic threshold effect can be advanced. For 400-W and 800-W incident powers, the results appear very similar, whereas for higher power, the percentage of damaged cells slowly decreases. This phenomenon could be explained by the exposure duration, which is shorter for highest powers. These remarks can complete the analyses provided by Shamis et al. (9) in their recent study. According to these authors, there is a possible specific effect of 18-GHz microwave radiation at sublethal temperatures on bacteria very similar to that of electroporation of the cell membrane and which appears to be electrokinetic in nature (9, 38).

Whereas a number of studies investigating the bactericidal effects of microwaves exist, few data on the specific effects of micro-

waves on prokaryotic cell membrane are available. In the electroporation theory (39), cell membrane pore formation generally results in cell material leakage and sometimes in cell lysis. The fact that no protein leakage was measured in DW-exposed samples was probably due to the low percentage of permeabilized cells. Moreover, the nature and extent of membrane damage might be insufficient to allow release of cell components, at least proteins. Those effects led us to think that DW exposure under the experimental conditions of this study might induce reversible membrane fluidity modification. Such a hypothesis could join that of a study by Orlando et al. (1994) of liposomes (40). These authors reported that microwaves could not induce membrane disruption but could induce pore formation. Consequently, the dielectric cell membrane rupture theory (41) may not be advanced to explain the DW-induced effects on membrane permeability. Instead of this theory, a phenomenon close to the electroporation theory appears more convincing. Although the mechanism by which electroporation occurs is incompletely understood, it is generally believed that a rapid structural rearrangement of the membrane occurs, whereby some or many aqueous pores perforate the membrane. When an imposed transmembrane potential reaches a threshold value, a rearrangement in the molecular structure of the membrane occurs, leading to the formation of pores and a substantial increase in cellular permeability to ions and molecules. Depending on the field strength and exposure time, the subsequent removal of the electric field may then allow the cell membrane to regain its structural integrity (9).

The temperature assessment is a key step in such experiments. Even if those experimental data suggested that the temperature reached by the microwave-exposed samples for the contact time studied was not high enough to explain the measured modification of cell membrane integrity, the heterogeneity should be considered.

This study focuses on characterization of microwave effects at the macroscopic level, corresponding to bulk solution measure-

ments. In such experiments, two kinds of temperatures can be considered: i) the bulk temperature, or the average fluid bulk temperature, which is a convenient reference point for evaluating properties related to convective heat transfer, and (ii) the instantaneous temperature, which is here a function of microwave power and is not directly measurable due to its short existence and molecular nature (38). As has been well discussed in a recent review from Shamis et al. (2012) (38), the instantaneous temperature principle suggests that a “nonthermal” effect cannot be considered to exist in microwave processing without careful control of this instantaneous temperature, since an unmeasured energy transfer is occurring between the microwaves and the sample. According to these authors, for microwave effects that cannot be accounted for by changes to bulk solution, the expression “specific microwave effects” may be more suitable than “nonthermal effects.”

Conclusion. This study showed that 2.45-GHz-DW exposure at 37°C induced *Escherichia coli* membrane modifications. The heating phase, in which the temperature increases from room level up to 37°C, appeared to be the most responsible for the measured effects of microwaves on membrane integrity. Increasing exposure times up to 30 min did not induce any increase in the percentage of permeabilized cells.

Approximately 8% of permeabilized cells appear after microwave exposure, while conventional heating at 37°C did not induce any effect. Moreover, the results showed that conventional heating at 47°C for 10 min or at 48°C for 5 min was necessary to induce the same effects. From these results, a direct link between the effect on membrane permeability and the temperature increase after microwave exposure cannot be established.

Thermal characterization during the heating step revealed clearly a heterogeneous temperature distribution in the cell suspension, but no spots above $45 \pm 1^\circ\text{C}$ were measured over the cell suspension volume. Even if those experimental data suggested that the temperature reached by the microwave-exposed samples for the contact time studied was not high enough to explain the measured modification of cell membrane integrity, the heterogeneity should be considered. The SAR distribution was computed for the whole sample. The results showed a nonhomogenous SAR distribution and highlight two SAR hot spots near the top and the bottom of the test tube (0.89 W/g at the maximum for 1-W incident power).

The results of this study seem to indicate that the cell response is power dependent: no effect was observed at 200 W, whereas significant effects were pointed out for power equal to or higher than 400 W. No more severe damage related to the applied power increase was observed over 400 W. From these results, the hypothesis of a specific electromagnetic threshold effect can be advanced.

This study focuses on characterization of microwave effects at the macroscopic level, corresponding to bulk solution measurements. In order to perform temperature measurements at the cellular level, further experiments based on the use of chemical reactions (42) and microfluorimetry techniques (43) would be carried out.

REFERENCES

1. Banik S, Bandyopadhyay S, Ganguly S. 2003. Bioeffects of microwave—a brief review. *Bioresour. Technol.* 87:155–159. [http://dx.doi.org/10.1016/S0960-8524\(02\)00169-4](http://dx.doi.org/10.1016/S0960-8524(02)00169-4).
2. de la Hoz A, Diaz-Ortiz A, Moreno A. 2007. Review on non-thermal effects of microwave irradiation in organic synthesis. *J. Microw. Power Electromagn. Energy* 41:44–64.
3. Ivaschuk OI, Jones RA, Ishida-Jones T, Haggren W, Adey WR, Phillips JL. 1997. Exposure of nerve growth factor-treated PC12 rat pheochromocytoma cells to a modulated radiofrequency field at 836.55 MHz: effects on c-jun and c-fos expression. *Bioelectromagnetics* 18:223–229. [http://dx.doi.org/10.1002/\(SICI\)1521-186X\(1997\)18:3<223::AID-BEM4>3.0.CO;2-4](http://dx.doi.org/10.1002/(SICI)1521-186X(1997)18:3<223::AID-BEM4>3.0.CO;2-4).
4. Koyama S, Takashima Y, Sakurai T, Suzuki Y, Taki M, Miyakoshi J. 2007. Effects of 2.45 GHz electromagnetic fields with a wide range of SARs on bacterial and HPRT gene mutations. *J. Radiat. Res.* 48:69–75. <http://dx.doi.org/10.1269/jrr.06085>.
5. Litovitz TA, Penafiel LM, Farrel JM, Krause D, Meister R, Mullins JM. 1997. Bioeffects induced by exposure to microwaves are mitigated by superposition of ELF noise. *Bioelectromagnetics* 18:422–430. [http://dx.doi.org/10.1002/\(SICI\)1521-186X\(1997\)18:6<422::AID-BEM4>3.0.CO;2-4](http://dx.doi.org/10.1002/(SICI)1521-186X(1997)18:6<422::AID-BEM4>3.0.CO;2-4).
6. George DF, Bilek MM, McKenzie DR. 2008. Non-thermal effects in the microwave induced unfolding of proteins observed by chaperone binding. *Bioelectromagnetics*. 29:324–330. <http://dx.doi.org/10.1002/bem.20382>.
7. Shazman A, Mizrahi S, Cogan U, Shimoni E. 2007. Examining for possible non-thermal effects during heating in a microwave oven. *Food Chem.* 103:444–453. <http://dx.doi.org/10.1016/j.foodchem.2006.08.024>.
8. Kim S-Y, Jo E-K, Kim H-J, Bai K, Park J-K. 2008. The effects of high-power microwaves on the ultrastructure of *Bacillus subtilis*. *Lett. Appl. Microbiol.* 47:35–40. <http://dx.doi.org/10.1111/j.1472-765X.2008.02384.x>.
9. Shamis Y, Taube A, Mitik-Dineva N, Croft R, Crawford RJ, Ivanova EP. 2011. Specific electromagnetic effects of microwave radiation on *Escherichia coli*. *Appl. Environ. Microbiol.* 77:3017–3022. <http://dx.doi.org/10.1128/AEM.01899-10>.
10. French PW, Donnellan M, McKenzie DR. 1997. Electromagnetic radiation at 835 MHz changes the morphology and inhibits proliferation of a human astrocytoma cell line. *Bioelectrochem. Bioenerg.* 43:13–18. [http://dx.doi.org/10.1016/S0302-4598\(97\)00035-4](http://dx.doi.org/10.1016/S0302-4598(97)00035-4).
11. Peinnequin A, Piriou A, Mathieu J, Dabouis V, Sebbah C, Malabiau R, Debouzy JC. 2000. Non-thermal effects of continuous 2.45 GHz microwaves on Fas-induced apoptosis in human Jurkat T-cell line. *Bioelectrochemistry* 51:157–161. [http://dx.doi.org/10.1016/S0302-4598\(00\)00064-7](http://dx.doi.org/10.1016/S0302-4598(00)00064-7).
12. Stagg RB, Thomas WJ, Jones RA, Adey WR. 1997. DNA synthesis and cell proliferation in C6 glioma and primary glial cells exposed to a 836.55 MHz modulated radiofrequency field. *Bioelectromagnetics* 18:230–236. [http://dx.doi.org/10.1002/\(SICI\)1521-186X\(1997\)18:3<230::AID-BEM5>3.0.CO;2-3](http://dx.doi.org/10.1002/(SICI)1521-186X(1997)18:3<230::AID-BEM5>3.0.CO;2-3).
13. Velizarov S, Raskmark P, Kwee S. 1999. The effects of radiofrequency fields on cell proliferation are non-thermal. *Bioelectrochem. Bioenerg.* 48:177–180. [http://dx.doi.org/10.1016/S0302-4598\(98\)00238-4](http://dx.doi.org/10.1016/S0302-4598(98)00238-4).
14. Goldblith SA. 1966. Basic principles of microwaves and recent developments, p 277–301. *In* Chichester CO, Mark EM, Stewart GF (ed), *Advances in food research*. Academic Press, New York, NY.
15. Chipley JR. 1980. Effects of microwave irradiation on microorganisms, p 129–145. *In* Perlman D (ed), *Advances in applied microbiology*. Academic Press, New York, NY.
16. Rosaspina S, Anzanel D, Salvatorelli G. 1993. Microwave sterilization of enterobacteria. *Microbios* 76:263–270.
17. Rosaspina S, Salvatorelli G, Anzanel D. 1994. The bactericidal effect of microwaves on *Mycobacterium bovis* dried on scalpel blades. *J. Hosp. Infect.* 26:45–50. [http://dx.doi.org/10.1016/0195-6701\(94\)90078-7](http://dx.doi.org/10.1016/0195-6701(94)90078-7).
18. Wu Q. 1996. Effect of high-power microwave on indicator bacteria for sterilization. *IEEE Trans. Biomed. Eng.* 43:752–754.
19. Atmaca S, Akdag Z, Dasdag S, Celik S. 1996. Effect of microwaves on survival of some bacterial strains. *Acta Microbiol. Immunol. Hung.* 43: 371–378.
20. Levre E, Valentini P. 1998. Inactivation of *Salmonella* during microwave cooking. *Zentralbl. Hyg. Umweltmed.* 201:431–436.
21. Woo I-S, Rhee I-K, Park H-D. 2000. Differential damage in bacterial cells by microwave radiation on the basis of cell wall structure. *Appl. Environ. Microbiol.* 66:2243–2247. <http://dx.doi.org/10.1128/AEM.66.5.2243-2247.2000>.
22. Dreyfuss MS, Chipley JR. 1980. Comparison of effects of sublethal microwave radiation and conventional heating on the metabolic activity of *Staphylococcus aureus*. *Appl. Environ. Microbiol.* 39:13–16.
23. Khalil K, Villota V. 1988. Comparative study on injury and recovery of *Staphylococcus aureus* using microwaves and conventional heating. *J. Food Prot.* 51:181.
24. Kozempel MF, Annous BA, Cook RD, Scullen OJ, Whiting RC. 1998.

- Inactivation of microorganisms with microwaves at reduced temperatures. *J. Food Prot.* 61:582–585.
25. Tajchakavit S, Ramaswamy HS, Fustier P. 1998. Enhanced destruction of spoilage microorganisms in apple juice during continuous flow microwave heating. *Food Res. Int.* 31:713–722. [http://dx.doi.org/10.1016/S0963-9969\(99\)00050-2](http://dx.doi.org/10.1016/S0963-9969(99)00050-2).
 26. Goldblith SA, Wang DIC. 1967. Effect of microwaves on *Escherichia coli* and *Bacillus subtilis*. *Appl. Microbiol.* 15:1371–1375.
 27. Fujikawa H, Ushioda H, Kudo Y. 1992. Kinetics of *Escherichia coli* destruction by microwave irradiation. *Appl. Environ. Microbiol.* 58:920–924.
 28. Cueille M, Collin A, Pivain C, Leveque P. 2008. Development of a numerical model connecting electromagnetism, thermal and hydrodynamics to analyse in vitro exposure system. *Ann. Telecommun.* 63:17–28. <http://dx.doi.org/10.1007/s12243-007-0007-0>.
 29. Barbesti S, Citterio S, Labra M, Baroni MD, Neri MG, Sgorbati S. 2000. Two and three-color fluorescence flow cytometric analysis of immunoidentified viable bacteria. *Cytometry* 40:214–218. [http://dx.doi.org/10.1002/1097-0320\(20000701\)40:3<214::AID-CYTO6>3.0.CO;2-M](http://dx.doi.org/10.1002/1097-0320(20000701)40:3<214::AID-CYTO6>3.0.CO;2-M).
 30. Bradford MM. 1976. A rapid and sensitive method for the quantitation of microgram quantities of protein utilizing the principle of protein-dye binding. *Anal. Biochem.* 72:248–254. [http://dx.doi.org/10.1016/0003-2697\(76\)90527-3](http://dx.doi.org/10.1016/0003-2697(76)90527-3).
 31. Ticaud N, Kohler S, Jarrige P, Duvillaret L, Gaborit G, O'Connor RP, Arnaud-Cormos D, Leveque P. 2012. Specific absorption rate assessment using simultaneous electric field and temperature measurements. *IEEE Antennas Wirel. Propag. Lett.* 11:252–255. <http://dx.doi.org/10.1109/LAWP.2012.2189748>.
 32. O'Connor RP, Madison SD, Leveque P, Roderick HL, Bootman MD. 2010. Exposure to GSM RF fields does not affect calcium homeostasis in human endothelial cells, rat pheochromocytoma cells or rat hippocampal neurons. *PLoS One* 5:e11828. <http://dx.doi.org/10.1371/journal.pone.0011828>.
 33. Leveque P, Reineix A, Jecko B. 1992. Modelling of dielectric losses in microstrip patch antennas: application of FDTD method. *Electron. Lett.* 28:539–541. <http://dx.doi.org/10.1049/el:19920340>.
 34. Kunz KKS, Luebbers RJ. 1993. The finite difference time domain method for electromagnetics. CRC Press, Boca Raton, FL.
 35. Taflove A, Hagness SC. 2005. Computational electrodynamics: the finite-difference time-domain method, 3rd ed. Artech House, Norwood, MA.
 36. Berenger J-P. 1994. A perfectly matched layer for the absorption of electromagnetic waves. *J. Comput. Phys.* 114:185–200. <http://dx.doi.org/10.1006/jcph.1994.1159>.
 37. Kappe PDCO, Stadler PDA. 2006. Microwaves in organic and medicinal chemistry. Wiley-VCH, Weinheim, Germany.
 38. Shamis Y, Croft R, Taube A, Crawford RJ, Ivanova EP. 2012. Review of the specific effects of microwave radiation on bacterial cells. *Appl. Microbiol. Biotechnol.* 96:319–325. <http://dx.doi.org/10.1007/s00253-012-4339-y>.
 39. Chang DC. 1992. Guide to electroporation and electrofusion. Academic Press, San Diego, CA.
 40. Orlando AR, Mossa G, D'Inzeo G. 1994. Effect of microwave radiation on the permeability of carbonic anhydrase loaded unilamellar liposomes. *Bioelectromagnetics* 15:303–313. <http://dx.doi.org/10.1002/bem.2250150405>.
 41. Zimmermann U, Pilwat G, Riemann F. 1974. Dielectric breakdown of cell membranes. *Biophys. J.* 14:881–899. [http://dx.doi.org/10.1016/S0006-3495\(74\)85956-4](http://dx.doi.org/10.1016/S0006-3495(74)85956-4).
 42. Nott KP, Hall LD. 1999. Advances in temperature validation of foods. *Trends Food Sci. Technol.* 10:366–374. [http://dx.doi.org/10.1016/S0924-2244\(00\)00023-6](http://dx.doi.org/10.1016/S0924-2244(00)00023-6).
 43. Copty AB, Neve-Oz Y, Barak I, Golosovsky M, Davidov D. 2006. Evidence for a specific microwave radiation effect on the green fluorescent protein. *Biophys. J.* 91:1413–1423. <http://dx.doi.org/10.1529/biophysj.106.084111>.